

Chapter 5

Design of Robust Controllers for Load Reduction in Wind Turbines

Asier Díaz de Corcuera, Aron Pujana-Arrese, Jose M. Ezquerra, Aitor Milo and Joseba Landaluze

Abstract This chapter proposes a methodology to design robust control strategies for wind turbines. The designed controllers are robust, multivariable and multi-objective to guarantee the required levels of stability and performance considering the coupling of the wind turbine. The proposed robust controllers generate collective pitch angle, individual pitch angle and generator torque control signals to regulate the electrical power production in the above rated power production zone and to mitigate the loads in the components of the wind turbines, like the drive train, tower, hub or blades, to increase their lifetime. The synthesis of these controllers is based on the H_∞ norm reduction and gain scheduling control techniques via Linear Matrix Inequalities. A wind turbine non-linear model has been developed in the GH Bladed software package and it is based on a 5 MW wind turbine defined in the Upwind European project. The family of linear models extracted from the linearization process of the non-linear model is used to design the proposed robust controllers. The designed controllers have been validated in GH Bladed and an exhaustive analysis has been carried out to calculate fatigue load reduction on wind turbine components, as well as to analyze load mitigation in some extreme cases.

A. Díaz de Corcuera (✉) · A. Pujana-Arrese · J.M. Ezquerra · A. Milo · J. Landaluze
IK4-IKERLAN, Arizmendiareta, 2, 20500 Arrasate-Mondragon,
The Basque Country, Spain
e-mail: adiazcorcuera@ikerlan.es

A. Pujana-Arrese
e-mail: apujana@ikerlan.es

J.M. Ezquerra
e-mail: jmezquerra@ikerlan.es

A. Milo
e-mail: amilo@ikerlan.es

J. Landaluze
e-mail: jlandaluze@ikerlan.es

Keywords Wind turbine · Robust control · Multivariable control · H_∞ control · Load mitigation

Nomenclature

A_n, B_n, C_n, D_n	State space matrices of system n
a_{Tfa}	Tower top fore-aft acceleration
a_{Tss}	Tower top side-to-side acceleration
C	Coleman transformation
C^{-1}	Anti-Coleman transformation
D_{ux}	Scalar constant in the control x channel
D_{ex}	Scalar constant in the output x channel
D_{dx}	Scalar constant in the disturbance x channel
e_{wg}	Generator speed error
K_{opt}	Optimum constant in below rated zone
M_{oop}	Blade root out-of-plane moment
M_{flap}	Blade root flapwise moment
M_{edge}	Blade root edgewise moment
M_{tilt}	Tilt moment in the rotor plane
M_{yaw}	Yaw moment in the rotor plane
p	Varying parameter
T	Generator torque
T_{DTD}	Torque contribution from drive train damping filter
T_{br}	Torque set-point in below rated zone
T_{sp}	Generator torque set-point
Unc	Uncertainty
w_g	Generator speed
β_{sp}	Pitch angle set-point
β_{col}	Collective pitch angle
B_{fa}	Pitch contribution from tower fore-aft damping filter
β_{tilt}	Pitch tilt angle in the rotor plane
β_{yaw}	Pitch yaw angle in the rotor plane
ψ	Azimuth angle
θ_T	Twist angle in the blade root section

5.1 Introduction

The continuous increase of the size of wind turbines, due to the demand of higher power production installations, has led to new challenges in the design of the turbines. Moreover, new control strategies are being developed. Today's strategies trend towards being multivariable and multi-objective, in order to fulfill the

numerous control design specifications in the non-linear and hardly coupled wind turbine system. To be more precise, one important specification is to mitigate loads in the turbine components to increase their life time.

This chapter presents different strategies to design robust, multivariable and multi-objective collective and individual blade pitch angle controllers and generator torque controllers. These controllers are based on the H_∞ norm reduction and gain scheduling control techniques to mitigate loads in wind turbines without affecting the electric power production. A wind turbine non-linear model has been developed using the GH Bladed software package and it is based on a 5 MW wind turbine defined in the Upwind European project [1]. The family of linear models extracted from the linearization process of the non-linear model is used to design the robust controllers. The designed controllers have been validated in GH Bladed and an exhaustive analysis has been carried out to calculate fatigue load reduction on wind turbine components, as well as to analyze load mitigation in some extreme cases.

The presented chapter is divided into four main sections, where the first one is this introduction. The second section presents general control concepts for wind turbines and the selected Upwind 5 MW wind turbine used to design the proposed controllers is briefly analyzed. Also, a baseline control strategy for the Upwind 5 MW based on classical control methods in wind turbines is carefully explained in this section. The third section shows the process to design the proposed multivariable robust controllers. These controllers are based on the research presented in [2] and they work in the above rated power production control zone. Their closed loop performance is analyzed in MATLAB. The designed robust controllers are:

- Generator Torque Controller based on the H_∞ norm reduction to mitigate the loads in the drive train and tower [3].
- Collective Pitch Controller based on the H_∞ norm reduction to mitigate loads in the tower and to regulate the generator speed at the nominal value [4]. The regulation of the generator speed is improved with a gain scheduling of three H_∞ controllers designed in three operating points. The gain scheduling is developed with a complex problem solved via Linear Matrix Inequalities (LMI).
- Individual Pitch Controller based on the H_∞ norm reduction [5] to mitigate loads in the tower and to align the rotor plane in the turbine.

The fourth section analyzes simulation results in GH Bladed using the different designed controllers compared to the baseline control strategy. Fatigue loads in DLC1.2 case and extreme loads in DLC1.6 and DLC1.9 cases are analyzed [6]. The last sections summarize the conclusions and the future of the work described in this chapter.

5.2 General Control Concepts for Wind Turbines

Wind turbines with generator variable speed regulation based on blade pitch angle control have been commonly used over the last few years by wind turbine manufacturers. The wind turbine control system is divided into two layers: the wind farm supervisory control, which generates external electric power demand set-points for each wind turbine, and the wind turbine supervisory control for each individual wind turbine. Furthermore, the wind turbine supervisory control is also divided into four operating states: startup, shutdown, park and power production. The control strategy in the electric power production zone is determined by a curve where the generator speed and the generator torque values are carefully related [7–9]. Figure 5.1 shows this curve for the 5 MW wind turbine explained in Sect. 5.2.1. The power production zone is defined by the curve $ABCD$ to be more time working at the optimum power coefficient value. The vertical sections AB and CD are implemented with generator torque controllers to regulate the generator speed at the references existing in the points A and C respectively. Between B and C points, the control zone is called below rated and it is implemented using a *look up table* control to work with the optimum power coefficient value while the pitch angle is fixed at the fine pitch angle, which is usually zero. However, in the D zone, the generator speed is regulated with a collective blade pitch angle control and the generator torque is kept at the nominal value. The transition between the generator torque control in the zone CD (transition zone) and the collective pitch control in zone D , called above rated, has to be soft to improve the controller performance [7, 10]. Sometimes, the rotor rotational frequencies $1P$, $2P$ and $3P$ are equal to other wind turbine structural modes in the tower, blades or drive train. If this coincidence exists, these modes can be dangerously excited. In [9, 11, 12], a strategy to avoid this coincidence is proposed, where the below rated zone is divided into five sub-zones: BE and GC to work in the power coefficient optimum value, EF and GH to regulate the generator speed outside the forbidden speed zone EG with a generator torque control.

Figure 5.2 shows the generator speed and electric power signals for the 5 MW wind turbine model in the different zones at the power production state. Also, the collective pitch angle and generator torque control signals are shown in next figures and they vary according to the wind operating point.

As it is mentioned in the introduction, the continuous increase of the size of wind turbines has led to new challenges in the design of wind turbine control systems beyond the main objective of electric power production. Today's control strategies trend towards being robust, multivariable and multi-objective in order to fulfill the numerous control design specifications considering the hardly coupling effects existing in a wind turbine non-linear system. One of the most important specifications is to mitigate loads in the turbine structural components. In spite of the coupling existing in wind turbines, classical control strategies for wind turbines in the power production zone uncouples the control problem into different Single Input Single Output (SISO) control loops to make easier the control system design:

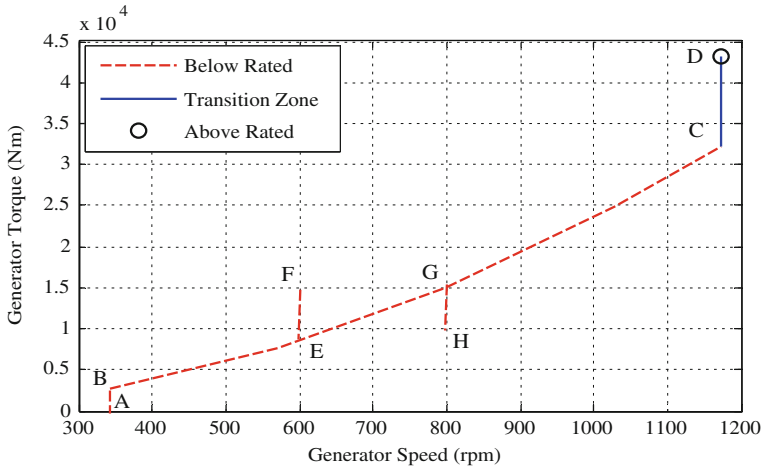


Fig. 5.1 Power production curve for upwind wind turbine

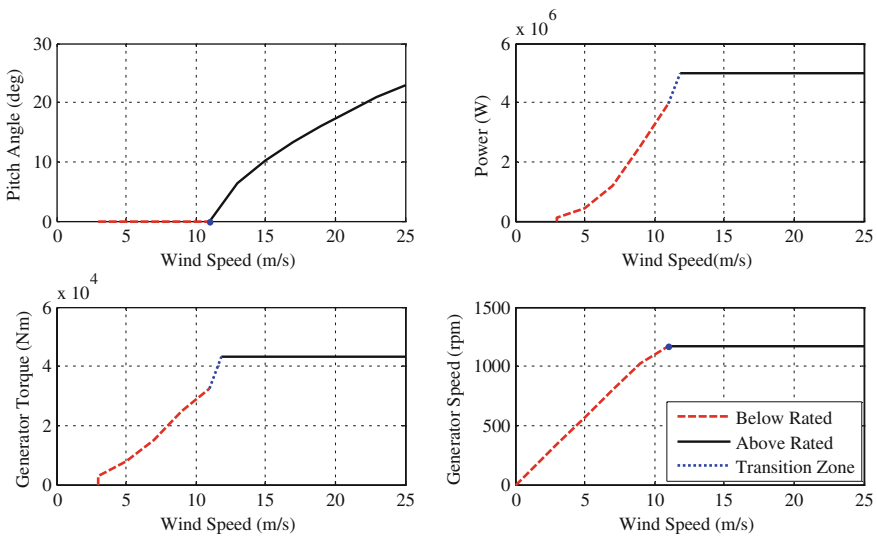


Fig. 5.2 Operating points for the upwind wind turbine

- Generator speed regulation varying the generator torque in *AB* and *CD* zones.
- Generator speed regulation varying the collective pitch angle in above rated zone.
- Drive train mode damping varying the generator torque to mitigate loads in the drive train.
- Tower fore-aft first mode damping varying the collective pitch angle and tower side-to-side first mode damping varying the generator torque to mitigate loads in the tower.

- Individual pitch angle control (IPC) to reduce loads caused by the misalignment of the rotor due to the stochastic dimensional wind, the wind shear, the yaw angle error and the tower shadow.

Over the last few years, several modern control techniques have been proposed to replace the classical SISO control loops with more complex Multi-Input Multi-Output (MIMO) controllers and to consider the real coupling existing in the wind turbine from a multi-objective control design point of view. These techniques are based on fuzzy control [13], adaptive control [14], Linear Quadratic control [15], QFT control [16], Linear Parameter Varying (LPV) control [17, 18] and control synthesis based on the H_∞ norm reduction [19]. H_∞ and LPV control techniques are robust and they can be multivariable and multi-objective, so their application in wind turbines offers a lot of advantages and interesting experimental results can be achieved using them [20]. Next section, where the design of different robust controllers is explained, is focused on two of these control techniques, control synthesis based on the H_∞ norm reduction and gain scheduling control techniques, and their application in the above rated power production zone of wind turbines, where the system non-linearities are more relevant.

The classical control design process for wind turbines is similar to the one used in other mechatronic systems and it is based on the design of a Linear Time Invariant (LTI) controller in different operating points of the non-linear model. Initially, the wind turbine non-linear model is needed to design and validate the controllers in simulation before experimental tests. The wind turbine non-linear model can be carried out from analytical models or making a closed loop identification of the system [21, 22]. Specific software packages exist to develop wind turbine complex analytical models (GH Bladed and FAST are the most well-known ones). GH Bladed [23] is commercialized by Garrad Hassan, whereas FAST [24] is an open source developed by the National Renewable Laboratory (NREL). Once the wind turbine is modeled as a non-linear system, this system is linearised in different operating points. Then, the generator torque and blade pitch angle controllers are designed in different operating points where they work. Finally, the designed controller performance is analyzed in the different operating points and they are discretized and tested using the initial non-linear model. The validation of the wind turbine control loops requires a load analysis based on the analysis of the fatigue damage and different extreme load cases [6].

5.2.1 Wind Turbine Non-Linear Model

The Upwind wind turbine defined inside the Upwind European project has been modelled in GH Bladed 4.0 software package and it is the reference wind turbine non-linear model used to design the controllers presented in this chapter. The Upwind model consists of a 5 MW offshore wind turbine [1] with a monopile structure in the foundation. It has three blades and each blade has an individual

pitch actuator. The rotor diameter is 126 m, the hub height is 90 m, it has a gear box ratio of 97, the rated wind speed is 11.3 m/s, the cut-out wind speed is 25 m/s and the rated rotor rotational speed is 12.1 rpm, so the nominal generator speed is 1,173 rpm. The family of linear models of this wind turbine is obtained in different operating points from the wind turbine non-linear model using the linearization tool of this software. Twelve operating points are defined according to wind speeds from 3 to 25 m/s. Once the non-linear model has been linearized, a modal analysis of the structural and non-structural modes of the wind turbine is essential to carry out a good control system. For example, the most important modes of the Upwind wind turbine in the operating points with wind speeds of 11 and 19 m/s are represented in Table 5.1. The 1P non-structural mode is related to the rotor rotational speed, which nominal value is 0.2 Hz for this wind turbine.

The plants of the family of linear models are expressed by the state-space matrices (Eq. 5.1) and they have different inputs and outputs. The inputs $u(t)$ are the collective pitch angle $\beta(t)$, the individual pitch angle in each blade $\beta_1(t)$, $\beta_2(t)$, $\beta_3(t)$, the generator torque control $T(t)$ and the disturbance input $w(t)$ caused by the wind speed. The outputs $y(t)$ are the sensorized measurements used to design the controller. The outputs used in the different designs shown in this chapter are the generator speed $w_g(t)$, the tower top fore-aft acceleration $a_{Tfa}(t)$, the tower top side-to-side acceleration $a_{Tss}(t)$ and the bending flapwise $M_{flap}(t)$ and the bending edgewise $M_{edge}(t)$ moments in the blade roots. Due to the non-linear model complexity, and the number of modes taken into account, the order of the linear models is 55.

$$\begin{aligned} \dot{x}(t) &= A_x x(t) + B_u u(t) + B_w w(t) \\ y(t) &= C_x x(t) + D_u u(t) + D_w w(t) \end{aligned} \quad (5.1)$$

Figure 5.3 shows the SISO family of linear plants of the Upwind wind turbine model which relates the collective pitch angle control signal to the measured generator speed. Three operating points in the above rated zone are presented to demonstrate the differences between them for wind speeds of 13, 19 and 25 m/s due the non-linearities of the wind turbine in this control zone.

5.2.2 Baseline Control Strategy

The baseline control strategy to regulate the electric power production for the Upwind 5 MW wind turbine developed in this chapter is based on the *ABCD* curve shown in Fig. 5.1 and the control loops explained in [10]. This strategy is named *C1* and it is used to be compared with the robust controllers described in next sections. In the below rated zone, the generator torque control depends on the generator speed measurement (Eq. 5.2). The generator torque T_{br} is proportional to the square of the generator speed by a constant K_{opt} , where K_{opt} is 2.14 Nm/(rad/s²) for the Upwind model. In this way, the wind turbine works with the optimum power coefficient value.

Table 5.1 Modal analysis for the upwind 5 MW wind turbine

Element	Mode	Frequency (Hz) at 11 m/s	Frequency (Hz) at 19 m/s
Rotor	In-plane 1st collective	3.68	3.69
	In-plane 2st collective	7.85	7.36
	Out-of-plane 1st collective	0.73	0.73
	Out-of-plane 2nd collective	2.00	2.01
Drive train	Drive train	1.66	1.63
Tower	1st tower side-to-side	0.28	0.28
	1st tower fore-aft	0.28	0.28
	2nd tower side-to-side	2.85	2.87
	2nd tower fore-aft	3.05	3.04
Non-structural	1P	0.2	0.2
	3P	0.6	0.6

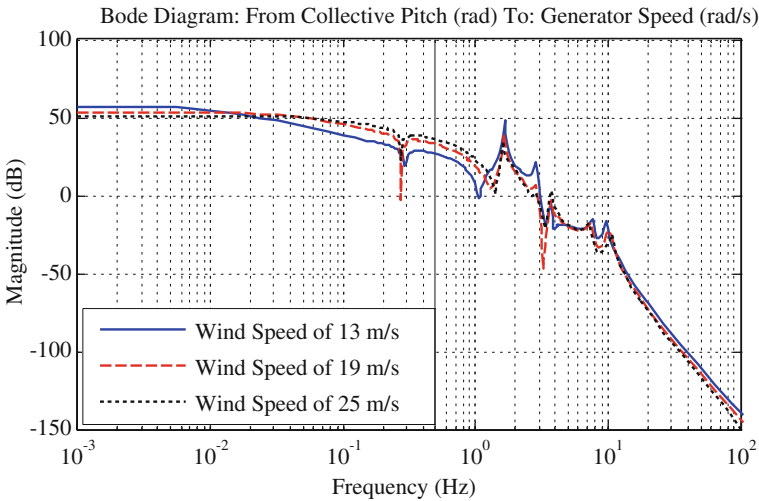


Fig. 5.3 Family of linear models for the upwind wind turbine

$$T_{br} = K_{opt} \cdot w_g^2 \tag{5.2}$$

A Drive Train Damping filter (DTD) is essential in the control design of wind turbines and it has to be firstly designed because the drive train mode is critically coupled in most control loops. The aim of the DTD is to damp the drive train mode and it has to be used in all control zones during the power production. The DTD used in the baseline control strategy for the Upwind model (Eq. 5.3) consists of

one gain, with one differentiator, one real zero and a pair of complex poles. In the designed DTD, K_1 is 641.45 Nms/rad, w_1 is 193 rad/s, w_2 is 10.4 rad/s and ζ_2 is 0.984.

$$T_{\text{DTD}}(s) = \left(K_1 \frac{s \left(1 + \frac{1}{w_1} s \right)}{\left(\left(\frac{1}{w_2} \right)^2 s^2 + 2\zeta_2 \frac{1}{w_2} s + 1 \right)} \right) w_g(s) \quad (5.3)$$

On the other hand, the objective in the transition zone is the regulation of generator speed varying the generator torque. In the baseline control strategy, it can be developed by using a proportional-integral (PI) controller (Eq. 5.4). In the baseline control strategy, called C1 in this chapter, the PI values in the transition zone (operating point with wind speed of 11 m/s) used in the Upwind baseline controller are w_T and K_T (Eq. 5.4), where $T(s)$ is the generator torque control signal, $e_{wg}(s)$ is the generator speed error. In this case, w_T is 0.5 rad/s and K_T is 2,685.2 Nm/rad.

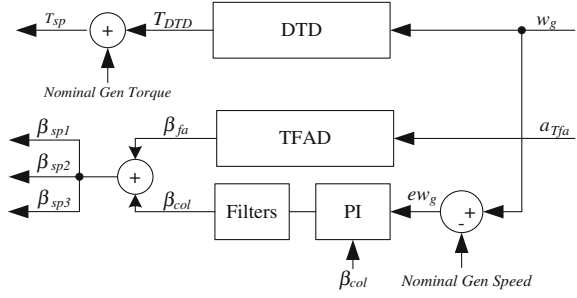
$$T(s) = K_T \frac{\left(1 + \frac{1}{w_T} s \right)}{s} e_{wg}(s) \quad (5.4)$$

The main objective in the above rated zone is the regulation of the generator speed control at the nominal value of 1,173 rpm varying the collective pitch angle in the blades and keeping the electric power at the nominal value of 5 MW. The control structure used in this baseline control strategy in the above rated zone is shown in Fig. 5.4. This regulation of the generator speed is based on a Gain-Scheduled (GS) collective pitch angle PI controller. In this case, the controller input $e_{wg}(s)$ is the generator speed error, and the controller output $\beta_{\text{col}}(s)$ is the collective pitch angle control signal. The linear plants used to tune the gain-scheduled PI controller are the plants which relate pitch angle and generator speed. These plants have different gains (see Fig. 5.3), so gain-scheduling is used to guarantee the stability of the closed loop system in spite of these differences. Two PI controllers (Eq. 5.5), in two operating points with wind speeds of 13 and 21 m/s, are designed and then a GS is applied to interpolate them. For 13 m/s, K_{B13} is 0.00158 and w_{B13} is 0.2 rad/s and, for 21 m/s, K_{B21} is 0.00092 and w_{B21} is 0.2 rad/s.

$$\beta_{\text{col}} = K_B \frac{\left(1 + \frac{1}{w_B} s \right)}{s} e_{wg}(s) \quad (5.5)$$

The gain scheduling interpolation is developed according to an average of the measured pitch angle in the blades. Nowadays, new sensors that provide information about the present wind speed in front of the hub of the wind turbine, like LIDARs [25], are being included in the pitch control systems improving the

Fig. 5.4 Baseline control strategy in the above rated zone



regulation of the generator speed and reducing the loads in the wind turbine. The corresponding steady-state collective pitch angle in the operating points where the collective pitch PI controllers are designed are 6.42° and 18.53° respectively. Next, some series notch filters are included in the regulation loop to improve the PI controller response [26]. Classical design criteria [27] are established to tune these controllers in these operating points, for instance: output sensitivity peak of 6 dB approximately, open loop phase margin between 30° and 60° , open loop gain margin between 6 and 12 dB and keeping constant the PI zero frequency.

Finally, a Tower Fore-Aft Damping filter (TFAD) is designed to reduce the wind effect in the tower fore-aft first mode in the above rated power production zone [28]. For the Upwind baseline controller, the filter (Eq. 5.6) consists of a gain with one integrator, a pair of complex poles and a pair of complex zeros. The input of the TFAD is the fore-aft acceleration measured in the tower top a_{Tfa} and the output is the pitch contribution β_{fa} to the collective pitch angle. For the designed TFAD, K_{TD} is 0.035, w_{T1} is 1.25 rad/s, ζ_{T1} is 0.69, w_{T2} is 3.14 rad/s and ζ_{T2} is 1.

$$\beta_{fa}(s) = K_{TD} \frac{1}{s} \left(\frac{1 + \left(\frac{2\zeta_{T1}s}{w_{T1}} \right) + \left(\frac{s^2}{w_{T1}^2} \right)}{1 + \left(\frac{2\zeta_{T2}s}{w_{T2}} \right) + \left(\frac{s^2}{w_{T2}^2} \right)} \right) a_{Tfa}(s) \quad (5.6)$$

As Fig. 5.4 shows, the individual pitch angle set-point to each blade β_{sp1} , β_{sp2} and β_{sp3} are equal and they are made up of the control signals β_{fa} and β_{col} , and the generator torque set-point T_{sp} is obtained adding the nominal generator torque in above rated and the torque contribution of the DTD filter T_{DTD} .

5.3 Design of Robust Controllers

The robust control design process for load reduction in wind turbines is shown in Fig. 5.5. The robust control techniques applied are based on the H_∞ norm reduction and gain scheduling interpolation. Initially, the non-linear model is linearized to extract the family of linear models. Next, the modal analysis is carried out to analyze the structural and non-structural modes of the system.

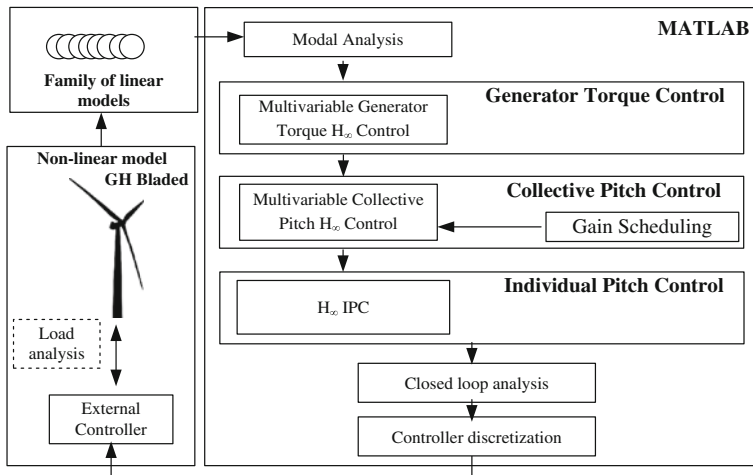


Fig. 5.5 Robust control design process for load reduction in wind turbines

The designed control loops are the generator torque control, the collective pitch control and the individual pitch control (IPC). Only one MIMO H_∞ control is proposed to develop the generator torque control. A MIMO H_∞ control and gain scheduling of different H_∞ controllers via LMI solution are proposed to carry out the collective pitch angle control. Also, a MIMO H_∞ control is finally proposed to perform a promising IPC. The controller design sequence is essential because the generator torque control has to be considered when designing the pitch angle control loops due to the couplings inherent to the system, mainly due to the hardly coupling of the drive train mode.

Once the controllers are obtained, they are reduced and validated by a closed loop analysis in different operating points with the family of linear models. Finally, they are discretized with a sample time of 0.01 s, which is commonly used by wind turbine manufacturers and, afterwards, they are included in the custom-written controller to work with the non-linear wind turbine model. A load analysis is carried out to analyze the load reduction in different components of the wind turbine. Table 5.2 shows the control objectives of the different proposed robust controllers in the above rated zone.

5.3.1 Design of H_∞ Robust Controllers

Controllers based on the H_∞ norm reduction are robust from the control design point of view, so their application is very powerful for control systems design due to the fact that real engineering systems are vulnerable to external disturbances and noise measurements and due to the differences between the real systems and the mathematical models. A controller design requires a fixed certain performance

Table 5.2 Objectives of the designed robust controllers

Order	Controller name	Control objectives
I	Generator torque H_∞ control	To reduce the wind effect in the drive train and tower side-to-side first modes
II	Collective pitch H_∞ control	To improve the regulation of the generator speed and to reduce the wind effect in the tower fore-aft first mode
III	Collective pitch gain scheduled control	To improve the regulation of the generator speed
IV	Individual pitch H_∞ control	To reduce the wind effect in the tower side-to-side first mode and to align the rotor plane

level when facing the disturbance signals, noise interferences, no-modelled plant dynamics and plant parameter variations. These design objectives can be achieved using a feedback control mechanism, but it introduces the need of sensors, bigger system complexity and a guarantee of system stability. Since the 80s, many authors researched the controller design using the H_∞ norm [29, 30] and the applications of these controllers in different non-linear real systems. Currently, the MATLAB Robust Toolbox [31] is a useful tool to solve mathematically the H_∞ controller synthesis problem.

The designed H_∞ controllers are LTI systems and the controller performance is defined using weight functions, scale constants [32] and defining a nominal plant among the family of linear plants where the controller synthesis is made. The most usual feedback control problem is expressed as a mixed sensitivity problem. The mixed sensitivity problem is based on a nominal plant and three weight functions and it can be considered in SISO or MIMO systems. These matrices of weight functions $W_1(s)$, $W_2(s)$ and $W_3(s)$ define the performance of the sensitivity functions $S(s)$, $T(s)$ and $U(s)$ respectively in a classical mixed sensitivity problem scenario (Fig. 5.6), where $S(s)$ is the output sensitivity, $T(s)$ is the input sensitivity and $U(s)$ is the control sensitivity. The scale constants are used to make the scaling of the different channels of the system. The difference between the family of plants can be modeled as uncertainties and they can be structured or unstructured. The unstructured uncertainties considered in the H_∞ robust control design are commonly modeled in different representations: additive uncertainty, input multiplicative uncertainty, output multiplicative uncertainty, inverse additive uncertainty, input inverse multiplicative uncertainty and output inverse multiplicative uncertainty. The selected one in this chapter is the additive representation. Finally, the calculation of the $K(s)$ controller based on the H_∞ norm reduction in this mixed sensitivity problem consists of the resolution of two *Riccati* equations, which can be solved with the MATLAB Robust control toolbox.

In the case of the wind turbine control design, two MISO (2×1) mixed sensitivity problems are necessary to design the MISO proposed generator torque and collective pitch controllers based on the H_∞ norm reduction. This control scenario is based on the augmented plant (Eq. 5.7) which is divided into the nominal plant $G(s)$, scale constants D_u , D_{d1} , D_{d2} , D_{e1} , D_{e2} and weight functions $W_{11}(s)$, $W_{12}(s)$, $W_2(s)$, $W_{31}(s)$ and $W_{32}(s)$. The nominal plant is the plant used to design the

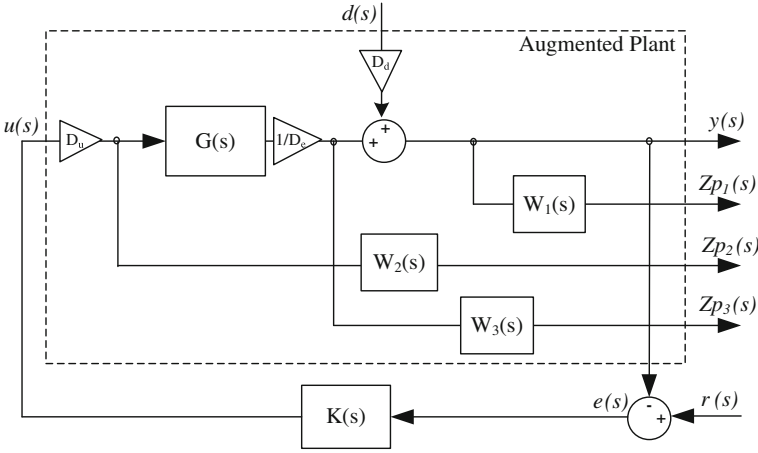


Fig. 5.6 Mixed control sensitivity problem

controller. The other plants of the family are considered as additive uncertainties in the pitch control design because these plants present differences. The inputs of the augmented plant are the output disturbances $d_1(s)$, $d_2(s)$ and the control signal $u(s)$. The outputs are the $y_1(s)$ and $y_2(s)$ from the scaled plant and the performance output channels $Z_{p11}(s)$, $Z_{p12}(s)$, $Z_{p2}(s)$, $Z_{p31}(s)$ and $Z_{p32}(s)$.

$$\begin{pmatrix} Z_{p11}(s) \\ Z_{p12}(s) \\ Z_{p2}(s) \\ Z_{p31}(s) \\ Z_{p32}(s) \\ y_1(s) \\ y_2(s) \end{pmatrix} = \begin{pmatrix} -(D_{d1}/D_{e1})W_{11}(s) & 0 & (D_u/D_{e1})G_{11}(s)W_{11}(s) \\ 0 & -(D_{d2}/D_{e2})W_{12}(s) & (D_u/D_{e2})G_{12}(s)W_{12}(s) \\ 0 & 0 & W_2(s) \\ 0 & 0 & (D_u/D_{e1})G_{11}(s)W_{31}(s) \\ 0 & 0 & (D_u/D_{e2})G_{12}(s)W_{32}(s) \\ -(D_{d1}/D_{e1}) & 0 & (D_u/D_{e1})G_{11}(s) \\ 0 & -(D_{d2}/D_{e2}) & (D_u/D_{e2})G_{12}(s) \end{pmatrix} \begin{pmatrix} d_1(s) \\ d_2(s) \\ u(s) \end{pmatrix} \tag{5.7}$$

5.3.1.1 Multivariable Generator Torque H_∞ Control

The H_∞ Torque Controller solves two of the control objectives: to reduce the wind effect in the drive train mode and to reduce the wind effect in the first tower side-to-side mode. The H_∞ Torque Controller has two inputs (generator speed w_g and tower top side-to-side acceleration a_{Tss}) and one output (generator torque $T_{H\infty}$).

The selected nominal plant to design the controller is the linearized plant at the 19 m/s wind speed operational point because it is a representative plant in the above rated zone. The nominal plant has the input of generator torque and two outputs: generator speed and tower top side-to-side acceleration. This nominal plant $G(s)$ (Eq. 5.8) is represented by the state space matrices A_{PT} , B_{PT} , C_{PT} and D_{PT} and it has 55 states. Uncertainties are not considered because the nominal plant is valid for all operating points in the above rated zone.

$$\begin{aligned} \dot{X}(t) &= A_{PT}X(t) + B_{PT}T(t) \\ \begin{pmatrix} w_g(t) \\ a_{Tss}(t) \end{pmatrix} &= C_{PT}X(t) + D_{PT}T(t) \end{aligned} \quad (5.8)$$

The nominal plant is generalized including the performance output channels and the scale constants (Eq. 5.9) D_u , D_{d1} , D_{d2} , D_{e1} , D_{e2} to scale the different channels of the mixed sensitivity scenario.

$$\begin{aligned} D_u &= 90 \\ D_{e1} &= 0.1; \quad D_{e2} = 1 \\ D_{d1} &= 0.1; \quad D_{d2} = 1 \end{aligned} \quad (5.9)$$

Finally, five weight functions are included in the generalized plant. In this mixed sensitivity problem, $W_{11}(s)$, $W_{12}(s)$, $W_2(s)$ are used. The weight functions $W_{31}(s)$ and $W_{32}(s)$ are not used, so their value is the unit when using the MATLAB Robust Toolbox. Like Fig. 5.7 shows, $W_{11}(s)$ is an inverted notch filter centered at the drive train frequency to mitigate the wind effect in this mode, $W_{12}(s)$ is an inverted notch filter centered at the tower side-to-side first mode to also mitigate the wind effect in this mode and $W_2(s)$ is an inverted low pass filter to reduce the controller activity in high frequencies.

After developing the controller synthesis, the obtained controller has to be re-scaled to adapt the input and the output to the real non-scaled plant. A high pass filter is included in the DTD channel if the input of the controller is changed to be the generator speed value instead of the generator speed error. The gain of this controller channel is reduced at low frequencies with this high pass filter. As it is defined in the augmented plant, the designed H_∞ Torque Controller has two inputs (generator speed in rad/s and tower top side-to-side acceleration in m/s^2) and one output (generator torque contribution T_{H_∞} in Nm). This designed controller is state space represented and its order is 39. Finally, the controller is reduced to order 25 without losing important information in its dynamics. After reducing, the last step is the controller discretization using a sample time of 0.01 s. The Bode diagram of the discretized state space represented controller (Eq. 5.10) is shown in Fig. 5.8.

$$\begin{aligned} X(k+1) &= A_{TD}X(k) + B_{TD} \begin{pmatrix} w_g(k) \\ a_{Tss}(k) \end{pmatrix} \\ T_{H_\infty}(k) &= C_{TD}X(k) + D_{TD} \begin{pmatrix} w_g(k) \\ a_{Tss}(k) \end{pmatrix} \end{aligned} \quad (5.10)$$

5.3.1.2 Multivariable Collective Pitch H_∞ Control

The H_∞ Pitch Controller solves two control objectives: the generator speed regulation increasing the output sensitivity bandwidth and reducing the output sensitivity peak compared to the classical control design, and to reduce the wind effect

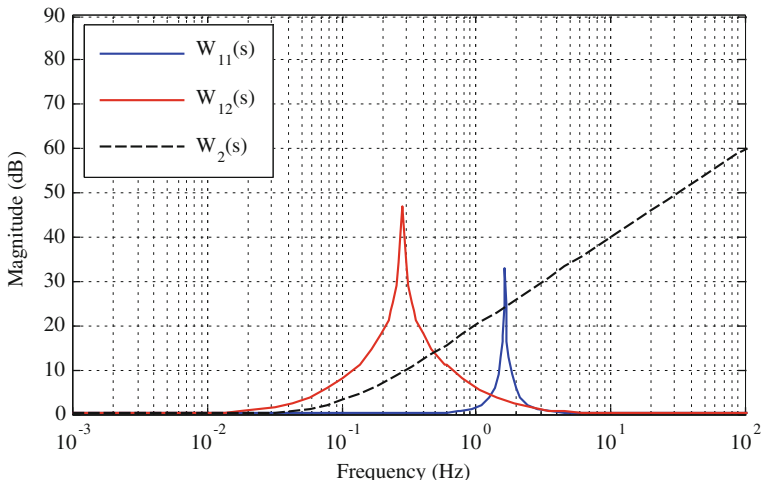


Fig. 5.7 Weight functions in the design of the generator torque H_∞ control

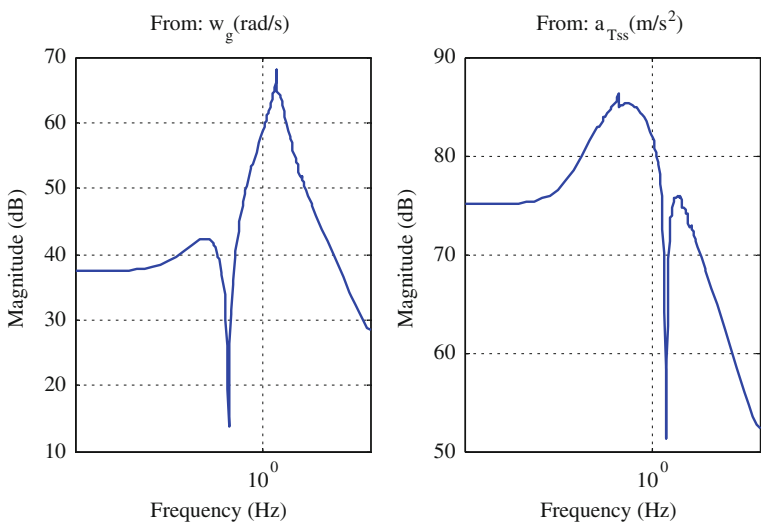


Fig. 5.8 Bode diagram of the generator torque H_∞ control

in the tower first fore-aft mode. Some notch filters are included in the pitch controller dynamics to reduce the excitation in some frequencies in the open loop response. The H_∞ Pitch Controller has two inputs (generator speed w_g and tower top fore-aft acceleration a_{TFa}) and one output (collective pitch angle β_{H_∞}).

The selected nominal plant to design the controller is the linealized plant at the 19 m/s wind speed operational point. The nominal plant has one input: collective pitch angle and two outputs: generator speed and tower top fore-aft acceleration.

This nominal plant $G(s)$ (Eq. 5.11) is represented by the state space matrices A_{PP} , B_{PP} , C_{PP} and D_{PP} and it has 55 states. The differences of the family of linear plants compared to the nominal plant are considered as additive uncertainties. These differences appear due to their non-linear behavior of the plant which relates the pitch angle and the generator speed.

$$\begin{aligned} \dot{X}(t) &= A_{PP}X(t) + B_{PP}\beta(t) \\ \begin{pmatrix} w_g(t) \\ a_{Tfa}(t) \end{pmatrix} &= C_{PP}X(t) + D_{PP}\beta(t) \end{aligned} \quad (5.11)$$

The nominal plant is generalized including the performance output channels and the scale constants D_u , D_{d1} , D_{d2} , D_{e1} , D_{e2} (Eq. 5.12) to scale the different channels of the MISO mixed sensitivity scenario.

$$\begin{aligned} D_u &= 1 \\ D_{e1} &= 10; \quad D_{e2} = 0.1 \\ D_{d1} &= 10; \quad D_{d2} = 0.1 \end{aligned} \quad (5.12)$$

Five weight functions are included to create the generalized plant. In this mixed sensitivity problem, the $W_{11}(s)$, $W_{12}(s)$, $W_2(s)$ are only used (see Fig. 5.10). $W_{11}(s)$ is an inverted high pass filter and it is used to define the closed loop output sensitivity performance, $W_{12}(s)$ is an inverted notch filter centered at the first tower fore-aft mode to mitigate the wind effect in this mode and $W_2(s)$ is an inverted low pass filter to reduce the controller activity in high frequencies. Some inverted notch filters are included in $W_2(s)$ to include notch filters in the controller dynamics. These filters are centered at the rotational frequencies $1P$ (0.2 Hz) and $3P$ (0.6 Hz) and at other structural modes.

The controller obtained by using the MATLAB Robust toolbox has to be re-scaled to adapt the inputs and output to the real non-scaled plant. The designed H_∞ Pitch Controller has two inputs (generator speed error in rad/s and tower top fore-aft acceleration in m/s^2) and one output (collective pitch angle β_{H_∞} in rad). This designed controller is state space represented and its order is 45. Finally, the controller is reduced to order 24 without losing important information in its dynamics. After reducing, the last step is the controller discretization using a sample time of 0.01 s. The Bode diagram of the discrete state space controller (Eq. 5.13) appears in Fig. 5.9.

$$\begin{aligned} X(k+1) &= A_{BD}X(k) + B_{BD} \begin{pmatrix} ew_g(k) \\ a_{Tfa}(k) \end{pmatrix} \\ \beta_{H_\infty}(k) &= C_{BD}X(k) + D_{BD} \begin{pmatrix} ew_g(k) \\ a_{Tfa}(k) \end{pmatrix} \end{aligned} \quad (5.13)$$

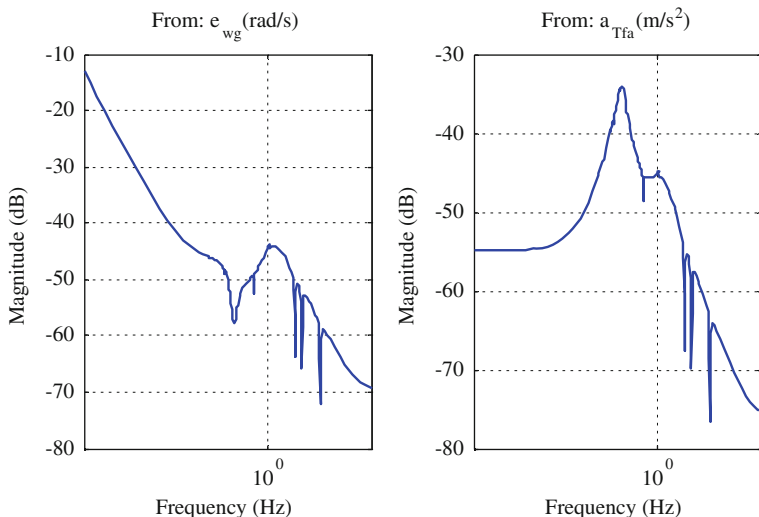


Fig. 5.9 Bode diagram of the collective pitch H_∞ control

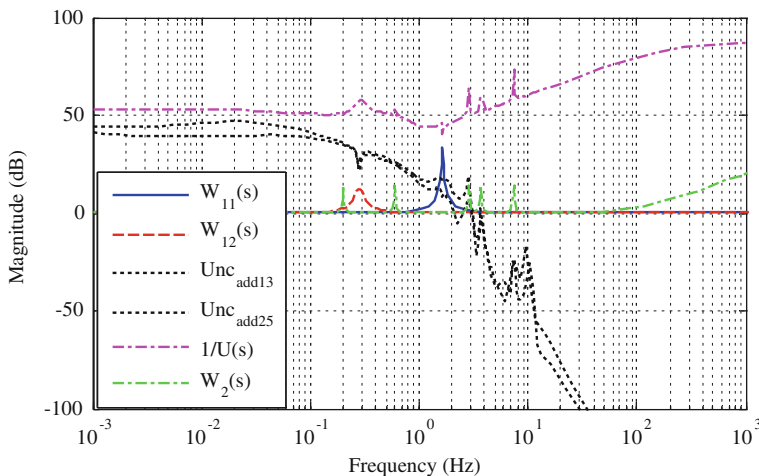


Fig. 5.10 Weight functions, uncertainties and control sensitivity function in the design of the collective pitch H_∞ control

After obtaining the pitch controller, the stability robustness of the closed loop for all plant in the family of linear models has to be analyzed. As it is proved in the small gain theorem [29], the inverse of the control sensitivity function has to be an upper limit of the modeled additive uncertainties (Fig. 5.10) to guarantee the robustness of the control in all operating points in the above rated zone.

Gain Scheduled Collective Pitch H_∞ Control

The interpolation of LTI controllers is an important task in control systems design for non-linear applications. In literature, the interpolation is commonly applied to low ordered LTI controllers and it can be divided into two approaches [33]: Gain Scheduling approach and LPV approach. The first one uses the family of linear models extracted from the non-linear model to design LTI controllers in different operating points to finally interpolate the designed controllers [34]. On the other hand, the LPV approach needs LPV models [35] of the plant to design LPV controls for the specified model [36]. The work presented in this section is focused on the first approach and it is based on gain scheduling of LTI controllers solving a LMI system. This technique guarantees the stability from the control design point of view because it is considered in the formulation of the LMI system. The adaptability of the presented gain scheduled control, which varies its behaviour according to the different operating points in wind turbines non-linear systems, improves the closed loop performance compared to LTI control techniques.

The non-linearities of wind turbines are more presented in the above rated zone, mainly in the pitch angle based generator speed regulation loop. To improve the control performance of the LTI H_∞ Pitch Controller, three collective pitch H_∞ controllers are designed to regulate the generator speed in three operating points in the above rated zone for wind speeds of 13, 19 and 25 m/s respectively. So, the above rated zone is divided into three sub-zones in this control design and each controller is optimized in performance for each zone guaranteeing the closed loop stability. Although the order of these controllers is high, they are perfectly interpolated without losing the stability and performance in all trajectories of the above rated zone solving an LMI system carefully proposed in [37]. The varying parameter p to develop the gain scheduling in the above rated zone is based on an adaptation of the measured pitch angle to work in the range $[-6, 6]$, which extreme points are calculated from the stationary pitch values of the operating points with wind speeds of [13 m/s, 25 m/s]. Figure 5.11 shows the bode diagram of discrete gain scheduling controller in three operating points where it is designed. The representation of the gain scheduled controller via LMI solution is based on a gain vector which interpolates the three state space LTI controllers previously adapted to make this interpolation.

5.3.1.3 Multivariable Individual Pitch H_∞ Control

One of the most well-known control loops developed to mitigate loads in wind turbines is the IPC. It consists of a controller which generates individual pitch set-points for each blade. The main objective of the IPC is to reduce the asymmetrical loads which appear in the rotor due to its misalignment caused by phenomena like wind shear, tower shadow, yaw misalignment or rotational sampling of turbulence. In [10, 38], decentralized d-q axes controllers based on proportional-integral (PI) controllers are proposed to solve this main objective using the

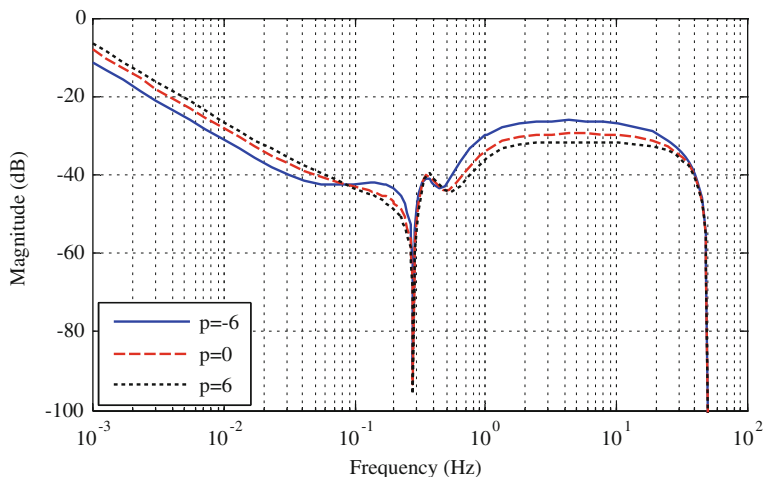


Fig. 5.11 Bode diagram of the gain scheduled collective pitch H_∞ controller in different operating points

Coleman transformation. The IPC to align the rotor frame has been field tested not only in the CART2 wind turbine [39], but it has also recently tested in the CART3 turbine with very promising results [40]. The load mitigation in the tower can be also considered as a control objective in the design of the Individual Pitch Controller. The tower side-to-side damping is commonly carried out with a generator torque contribution from measured side-to-side nacelle acceleration. This torque contribution affects to the quality of the generated electric power. In [41–43], different control strategies based on IPC are proposed to make the tower side-to-side damping with IPC signals. The interaction between the supervisory control and the IPC of the wind turbine is very important to reduce the loads in some components for shutdown and load sensor failure cases [10].

The IPC presented in this section, called H_∞ IPC, is composed of one MIMO controller based on the H_∞ norm reduction to generate individual pitch set-point signals for each blade with a multi-objective point of view (to align the rotor plane and to reduce the wind effect in the tower side-to-side first mode).

The first step when designing the H_∞ IPC is to create the nominal plant which will be included in the mixed sensitivity problem to make the H_∞ controller synthesis. To create this plant, firstly, the flapwise and edgewise moments extracted from strain gauges in the blade roots are transformed [44] to the out-of-plane moment M_{oop} using the transformation T (Eq. 5.14), where θ_T and β are the twist and pitch angles at the blade root section. The M_{tilt} and M_{yaw} rotor tilt and yaw moments are obtained using the transformation (Eq. 5.15) where ψ is the azimuth angle in each blade and M_{oop1} , M_{oop2} and M_{oop3} the out-of-plane moments in each blade. The tilt and yaw moments show how the blade loads developed in a rotating reference frame are transferred to a fixed reference frame. In this case, the Coleman transformation [45] C is used, and it is a transformation from a rotating to

a fixed reference frame, so M_{tilt} and M_{yaw} are proportional to the Coleman transformation outputs and the controller can be easily scaled. The inverse of the Coleman transformation C^{-1} is used to transform the fixed frame to the frame in blades.

$$\begin{aligned} \begin{pmatrix} M_{\text{oop1}} \\ M_{\text{oop2}} \\ M_{\text{oop3}} \end{pmatrix} &= \begin{pmatrix} \cos(\theta_T + \beta) & \sin(\theta_T + \beta) & 0 & 0 & 0 & 0 \\ 0 & 0 & \cos(\theta_T + \beta) & \sin(\theta_T + \beta) & 0 & 0 \\ 0 & 0 & 0 & 0 & \cos(\theta_T + \beta) & \sin(\theta_T + \beta) \end{pmatrix} \begin{pmatrix} M_{\text{flap1}} \\ M_{\text{edge1}} \\ M_{\text{flap2}} \\ M_{\text{edge2}} \\ M_{\text{flap3}} \\ M_{\text{edge3}} \end{pmatrix} \\ &= T \begin{pmatrix} M_{\text{flap1}} \\ M_{\text{edge1}} \\ M_{\text{flap2}} \\ M_{\text{edge2}} \\ M_{\text{flap3}} \\ M_{\text{edge3}} \end{pmatrix} \end{aligned} \quad (5.14)$$

For the ‘Upwind’ model $\cos(\theta_T + \beta) = 0.8716$ and $\sin(\theta_T + \beta) = 0.4903$

$$\begin{pmatrix} M_{\text{tilt}} \\ M_{\text{yaw}} \end{pmatrix} = \begin{pmatrix} \cos \psi_1 & \cos \psi_2 & \cos \psi_3 \\ \sin \psi_1 & \sin \psi_2 & \sin \psi_3 \end{pmatrix} \begin{pmatrix} M_{\text{oop1}} \\ M_{\text{oop2}} \\ M_{\text{oop3}} \end{pmatrix} \quad (5.15)$$

$$P_{\text{ipc}} = C^{-1}PTC = PT \quad (5.16)$$

The new plant P_{ipc} (Eq. 5.16) uses the mathematical properties of the Coleman transformation to simplify the construction of the plant. P_{ipc} has three outputs (a_{Tss} , M_{tilt} and M_{yaw}) and two inputs (β_{tilt} and β_{yaw}). The plant P_{ipc} linearized at the operating point of 19 m/s is used in the H_∞ IPC control design.

In this case, one MIMO (3×2) mixed sensitivity problem is necessary to design a MIMO controller based on the H_∞ norm reduction. The scale constants are shown in (Eq. 5.17). The weight functions used in this mixed sensitivity problem are $W_{11}(s)$, $W_{12}(s)$, $W_{13}(s)$, $W_{21}(s)$ and $W_{22}(s)$. The weight functions $W_{31}(s)$, $W_{32}(s)$, $W_{33}(s)$ are not used, so their value is the unit when using the MATLAB Robust Toolbox. Regarding to the weigh functions, $W_{11}(s)$ is an inverted notch filter centered at the tower first side-to-side mode frequency to reduce the wind effect in this mode, $W_{12}(s)$ and $W_{13}(s)$ are inverted high pass filters to guarantee the integral control activity to regulate the tilt and yaw moments. $W_{21}(s)$ and $W_{22}(s)$ are inverted low pass filters to reduce the controller activity in high frequencies with an inverted notch filter at the first blade in-plane mode frequency to include a notch filter at this frequency in the controller dynamics. Figure 5.12 shows the Bode diagrams of these weight functions.

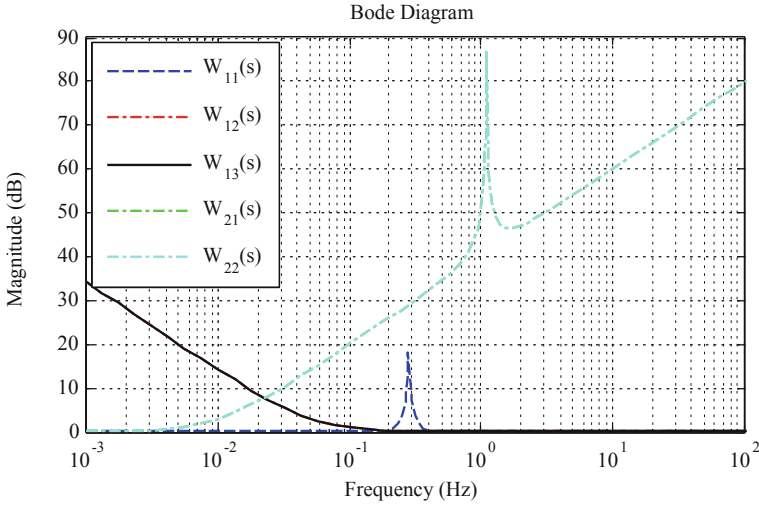


Fig. 5.12 Weight functions in the design of the individual pitch H_∞ control

$$\begin{aligned}
 D_{u1} &= 0.001; D_{u2} = 0.001; \\
 D_{d1} &= 0.1; D_{d2} = 1e6; D_{d3} = 1e6; \\
 D_{e1} &= 0.1; D_{e2} = 0.5e6; D_{e3} = 0.5e6;
 \end{aligned} \tag{5.17}$$

After finishing the controller synthesis, the obtained controller has to be re-scaled to adapt the inputs and the outputs to the real non-scaled plant. The designed H_∞ IPC controller has three inputs (tower top side-to-side acceleration a_{Tss} in m/s^2 , tilt moment in the rotor M_{tilt} in Nm and yaw moment in the rotor M_{yaw} in Nm) and two outputs (pitch angle in the rotor reference frame β_{ilt} in rad and yaw pitch angle β_{yaw} in the rotor reference frame in rad). This designed controller is state space represented and its order is 54. The reduction of the order of multivariable controllers is difficult due to coupling between the channels, so this controller is not reduced. The last step is the controller discretization with a sample time of 0.01 s. The Bode diagram of the discretized state space represented controller (Eq. 5.18) is shown in Fig. 5.13. Finally, the Coleman and its inverse have to be included in the control strategy to calculate the individual pitch angle contribution for each blade β_{rot1} , β_{rot2} and β_{rot3} . Figure 5.14 shows the complete control scheme of the IPC strategy from the signals from the loads in the blade roots to the individual pitch angle contributions. These pitch contributions for each blade are added to the collective pitch angle set-point obtained in the previously designed collective pitch angle controllers.

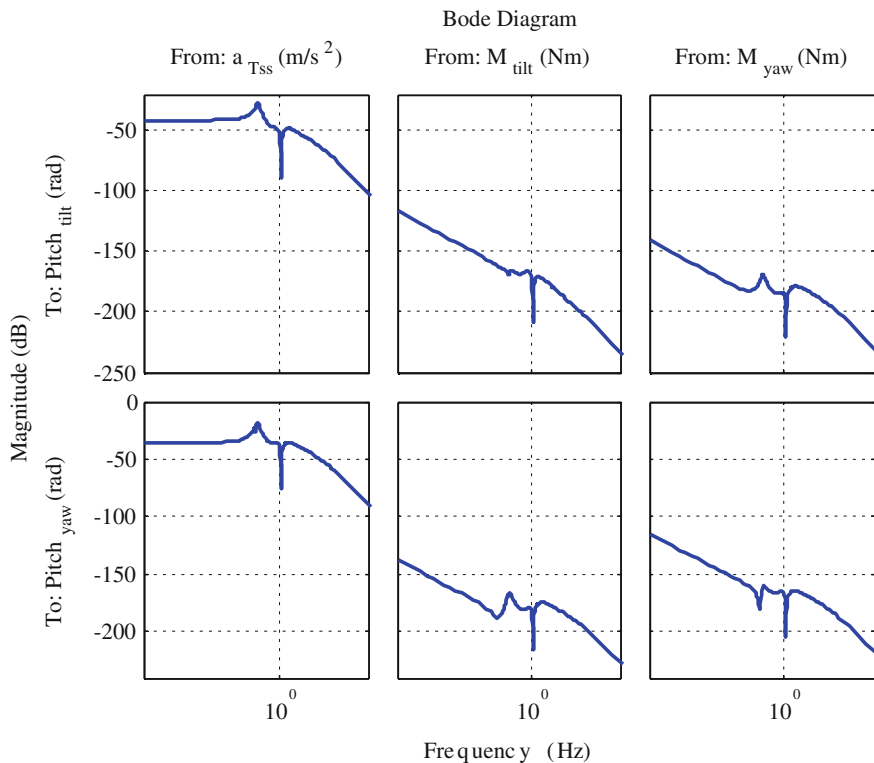


Fig. 5.13 Bode diagram of the individual pitch H_∞ control

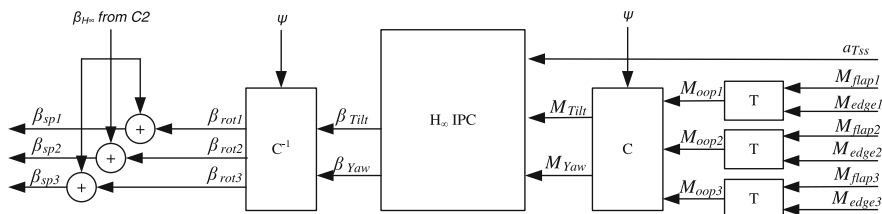


Fig. 5.14 Diagram of the individual pitch control strategy

$$\begin{aligned}
 x(k+1) &= A_{ipc1}x(k) + B_{ipc1} \begin{pmatrix} a_{Tss}(k) \\ M_{tilt}(k) \\ M_{yaw}(k) \end{pmatrix} \\
 \begin{pmatrix} \beta_{tilt}(k) \\ \beta_{yaw}(k) \end{pmatrix} &= C_{ipc1}x(k) + D_{ipc1} \begin{pmatrix} a_{Tss}(k) \\ M_{tilt}(k) \\ M_{yaw}(k) \end{pmatrix}
 \end{aligned}
 \tag{5.18}$$

5.3.2 Closed Loop Analysis of the Designed Robust Controllers

The closed loop analysis is an important step before including the designed controllers to work with the wind turbine non-linear model. Some control structures based on the designed controllers in this chapter are proposed to be analyzed not only in this closed loop analysis, but they will be also analyzed in the simulations shown in next section with the non-linear model. In all structures, the control strategy in the below rated zone is the same (baseline) but they present important differences in the above rated zone. These control structures in the above rated zone are:

- C1 Baseline control strategy based on gain scheduled PI pitch controller with DTD and TFAD filters
- C2 Robust control strategy based on two MISO H_∞ MISO LTI controllers: H_∞ Pitch Controller and H_∞ Torque Controller (see Fig. 5.15)
- C3 Robust control strategy based on two controllers. The generator torque control is the same as in C2. However, the collective pitch control is based on the gain scheduling of three H_∞ controllers via LMIs resolution (see Fig. 5.15)
- C4 It is an extension of the C2 robust control strategy with an extra-pitch angle contribution in each blade from the MIMO IPC H_∞ IPC (see Fig. 5.14)

The first analysis of the closed loop studies the output sensitivity function of the generator speed regulation loop. Table 5.3 shows the peaks and the bandwidth of this function in different operating points with the collective pitch angle controllers included in the control strategies C1, C2 and C3. The gain scheduled controller provides a larger bandwidth in the output sensitivity function, mainly at parameter values between -4 and 4 , with an interesting decrease of the output sensitivity peak in all operational points. This is a good performance from a load mitigation point of view in wind turbines, mainly for extreme changes of wind.

The damping of the drive train mode is very important and it can be developed using the baseline DTD filter in C1 or with the H_∞ Torque Controller in C2, C3 and C4. Figure 5.16 shows the bode diagram of the response of the generator speed from the generator torque control signal with these generator torque controllers in the operating point of 19 m/s. The drive train mode is perfectly damped with C1 and C2.

Figures 5.17, 5.18, 5.19 and 5.20 show the wind effect in different controlled signals of the wind turbine with the different control schemes at the operating point of 19 m/s. Figure 5.17 shows the wind effect in the generator speed. The regulation of this variable is better using the C3 control strategy at 19 m/s operating point due to the high bandwidth of this control loop (Table 5.3). Figure 5.18 shows the mitigation of wind effect in the tower fore-aft first mode with the C1 and C2 control strategies. Figure 5.19 shows the ability of mitigating the wind effect in the tower side-to-side first mode with a generator torque control in C2 control strategy or with an individual pitch controller developed in the C4 strategy. Finally, Fig. 5.20 shows the regulation of the rotor tilt moment using the IPC included in the C4 control scheme. Similar regulation is achieved in the rotor yaw moment with this strategy.

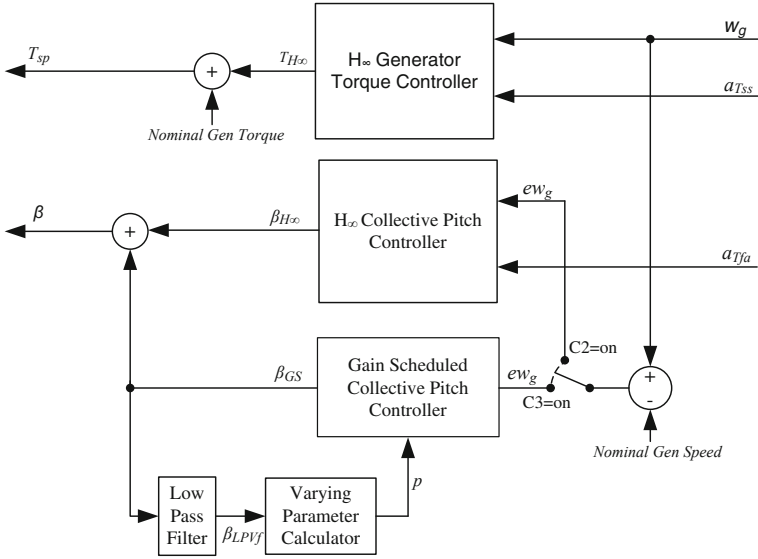


Fig. 5.15 Diagram of C2 and C3 control strategies

Table 5.3 Frozen output sensitivity analysis

Wind speed (m/s)	p value	Output sensitivity peak (dB)			Output sensitivity bandwidth (Hz)		
		C1	C2	C3	C1	C2	C3
13	-6	6.06	3.35	2.52	0.037	0.035	0.037
15	-4	6.06	3.59	2.87	0.045	0.044	0.059
17	-2	6.09	4.31	3.12	0.052	0.057	0.074
19	0	6.31	5.29	3.31	0.058	0.070	0.085
21	2	6.00	5.78	3.50	0.061	0.078	0.090
23	4	6.05	6.70	3.67	0.065	0.089	0.097
25	6	6.04	7.84	3.93	0.069	0.10	0.105

5.4 Simulation Results in GH Bladed

The control schemes explained in the closed loop analysis are included in the External Controller [46] in GH Bladed and different simulations are carried out using the *Upwind* non-linear wind turbine model with special wind conditions. The simulation analysis with the non-linear model is divided into two main steps:

- The analysis of a power production wind in above rated zone, in this case with a mean wind speed of 19 m/s, to see the time domain response of regulated signals. Also, the Power Spectral Density (PSD) of different signals within the

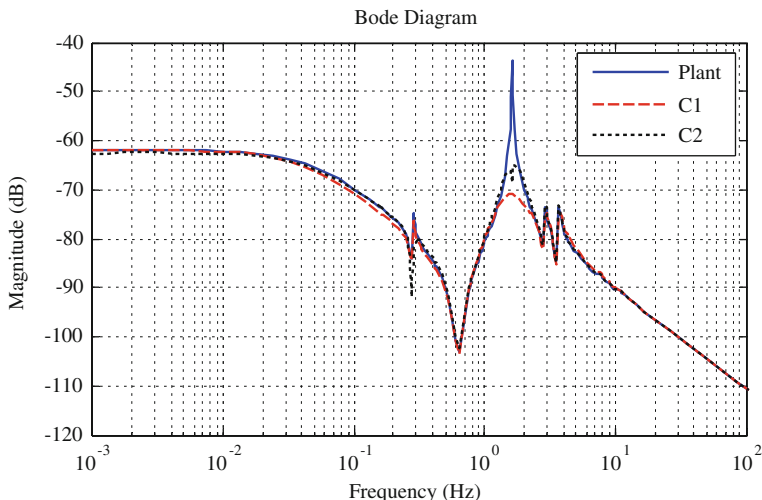


Fig. 5.16 Bode diagram of the plant “From: Generator Torque To: Generator Speed”

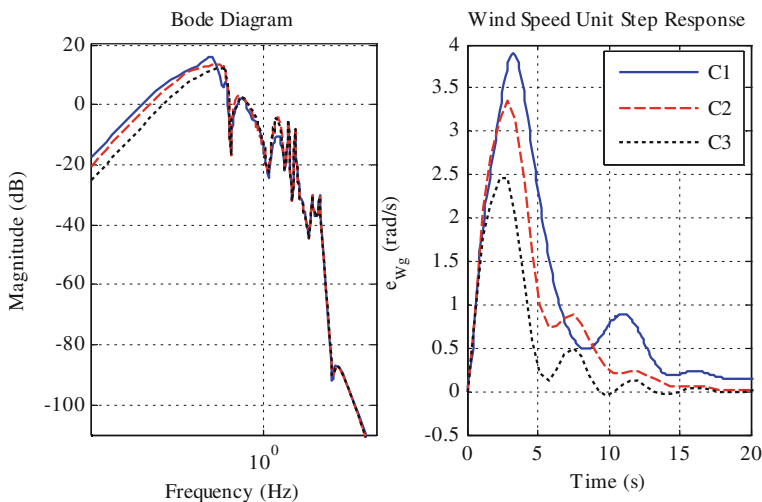


Fig. 5.17 Response of the generator speed for a wind input

control system is analyzed to see the control influence in the frequency domain representation of these signals.

- The load analysis to see the extreme and fatigue load mitigation achieved with these control strategies. The rain flow counting algorithm [47, 48] is used to carry out the load equivalent analysis to determine the fatigue damage on the

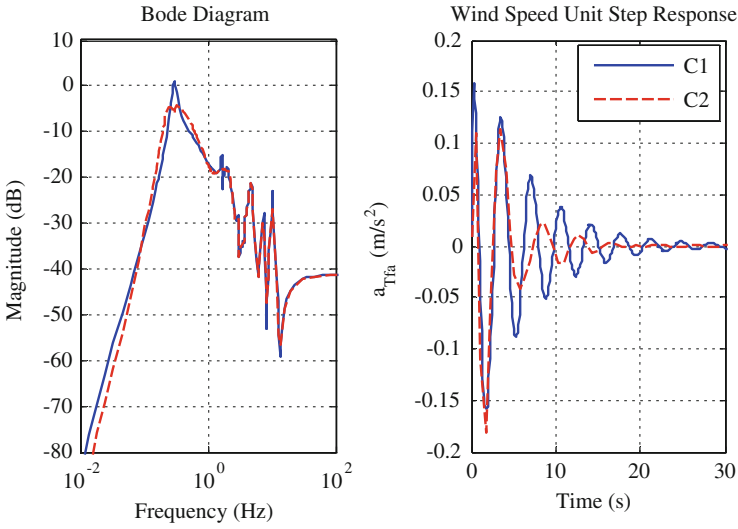


Fig. 5.18 Response of the tower top fore-aft acceleration for a wind input

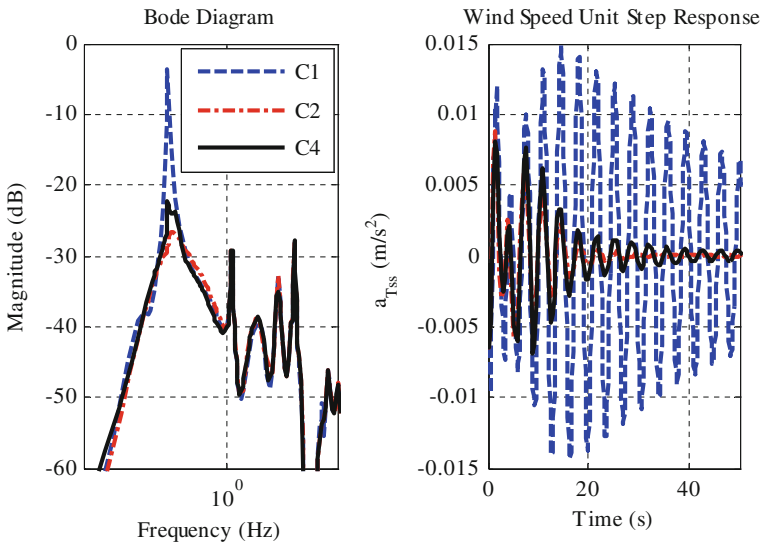


Fig. 5.19 Response of the tower top side-to-side acceleration for wind input

wind turbine components according to the constant of material m . The wind scenarios used to develop the fatigue analysis are based on 12 simulations of 600 s with power productions wind speeds with averages from 3 to 25 m/s. Also, a statistical analysis is usually carried out to see the mean and standard deviation of different signals in the wind turbine according to these twelve

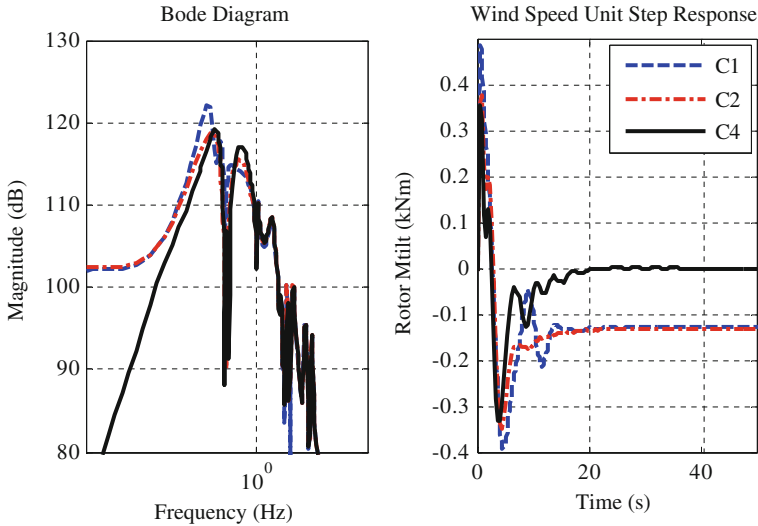


Fig. 5.20 Response of the rotor tilt moment for wind input

power production winds. On the other hand, two extreme load cases are analyzed: DLC1.6 and DLC1.9 cases. In these two analyses, the wind inputs are different gusts and ramps respectively. Other extreme load cases are not taken into account because results depend especially on the stop strategy, which has not been very affected by the designed robust controllers.

According to the first step in the simulation analysis, one simulation is carefully analyzed. The input of this simulation is a turbulent power production wind with a mean speed of 19 m/s (Fig. 5.21). The increase of the bandwidth of the output sensitivity function in the pitch control loop achieved using the robust controllers, mainly with the gain scheduled control in C3 (see Table 5.3), improves the regulation of the generator speed near to the nominal value of 1,173 rpm for this wind input (Fig. 5.22).

Different signals are also analyzed in the frequency domain using the PSD analysis. Figures 5.23 and 5.24 are focused on showing the influence of the designed feedback robust control loops to load mitigation in wind turbines in different variables. In this case, the C3 control strategy is not considered because the improvement in the generator speed regulation does not considerably affect to the load mitigation in power production wind cases. Figure 5.23 shows the pitch contribution of the IPC in the pitch control angle set-points using C4 control scheme. In this figure, the generator torque oscillations are reduced when the tower side-to-side first mode damping is developed using the IPC instead of with the generator torque control in C2 control strategy. The quality of the generated electric power is better if the oscillations in the torque control are avoided using C4 because the regulation of the generator speed is not affected by the pitch contributions in each blade generated with the IPC.

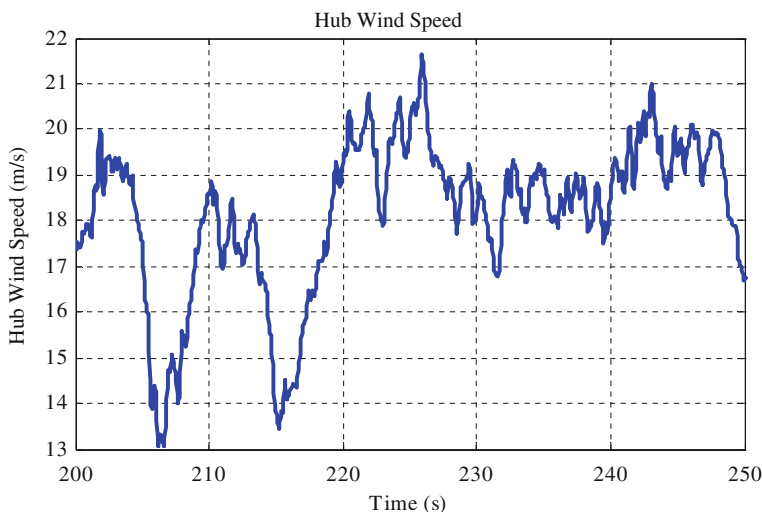


Fig. 5.21 Speed of the power production wind with mean of 19 m/s

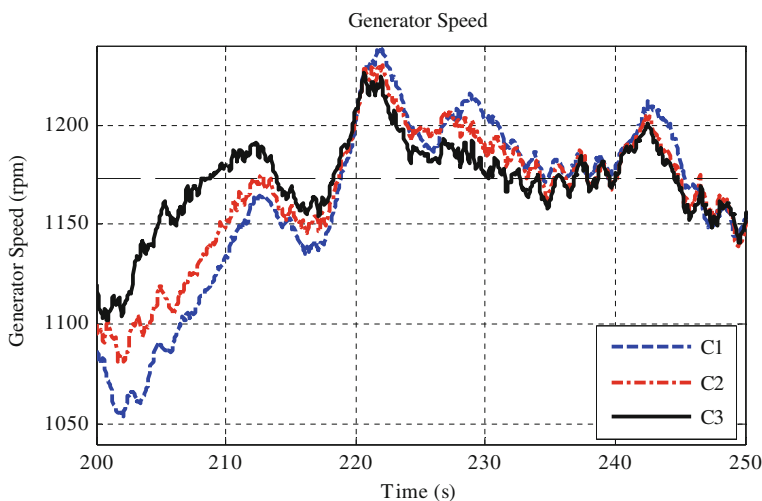


Fig. 5.22 Generator speed regulation for the power production wind

Figure 5.24 shows some important moments in different components of the wind turbine. The co-ordinate systems of blades, tower and hub are explained in [46]. The C4 control strategy reduces the activity at the $1P$ frequency in the blade out-of-plane moment M_{oop} and mitigates the activity of the M_{flap} moment around $1P$. However, the M_{edge} moment hardly depends on the $1P$ frequency and it is very difficult to mitigate loads in this variable. If the pitch actuator bandwidth was bigger, the activity of the blade first in-plane moment at 1.1 Hz in M_{edge} could be

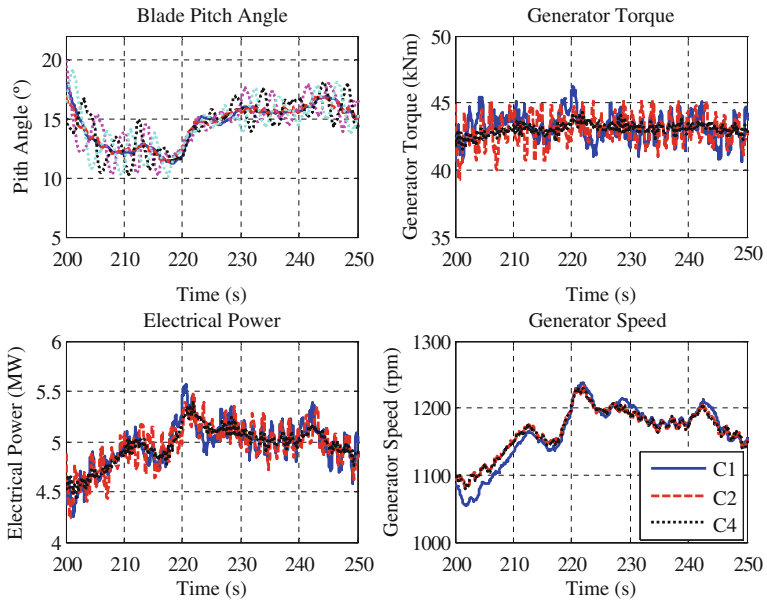


Fig. 5.23 Different signals for the power production wind

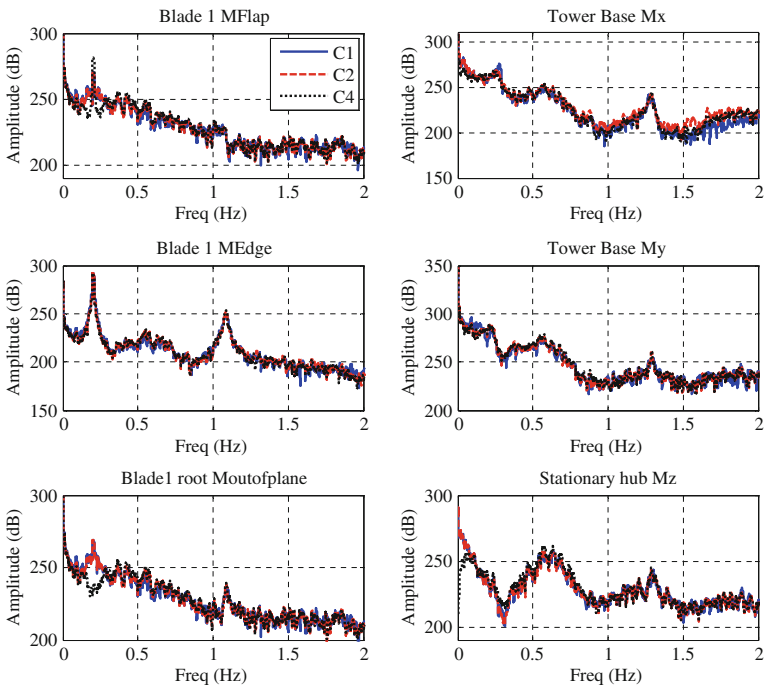


Fig. 5.24 Moments in different components for the power production wind speed

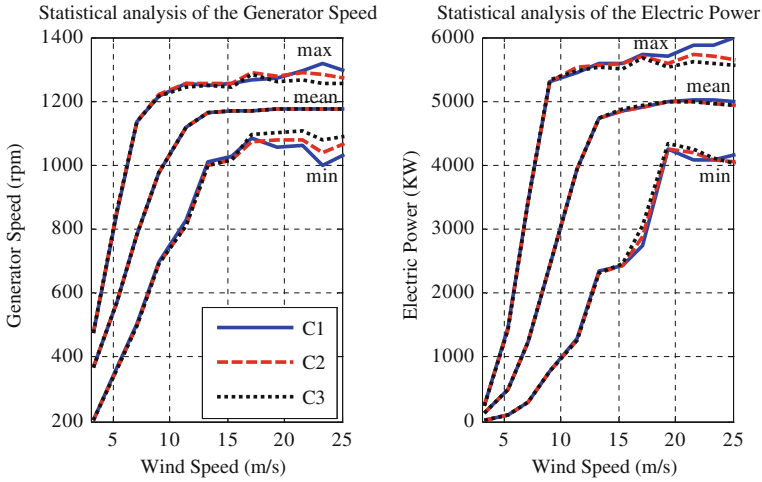


Fig. 5.25 Statistical analysis

reduced, but the pitch actuator bandwidth of the ‘Upwind’ model is only 1 Hz. The activity of the tower base moment in x is reduced with the $C4$ control strategy at the tower side-to-side first frequency, and the stationary hub moment in z is hardly mitigated at small frequencies due to the correct alignment of the rotor plane with IPC.

Figure 5.25 shows an statistical analysis of the regulated variables of generator speed and electric power. The maximum, minimum and mean values of these signals in different power production wind simulations are represented in Fig. 5.25. The regulation of the generator speed is better using $C3$ control scheme because the maximum and minimum values are closer to the nominal generator speed than with other strategies. Inherently, the regulation of the electric power is also better using $C3$ in spite of the difference in the generator torque control loop.

Table 5.4 represents the fatigue analysis with the four control schemes. $C1$ is considered as the reference to calculate the percentage of fatigue load reduction in different moments in the wind turbine components with the other control strategies. The m constant of material is 3 for the tower, m is 9 for the hub and for the yaw system and m is 12 for the blades. The inclusion of the generator torque contribution using the H_∞ torque controller in $C2$ reduces the fatigue load in the tower base moment in x axis in 11.9 % without important load increase in other components. The improvement in the generator speed regulation using $C3$ does not involve enhanced profits in the fatigue load analysis. On the other hand, the IPC based feedback control loop included in the $C4$ control strategy considerably affects to the fatigue loads. The fatigue loads are reduced in 7.5, 5.9, 5.3 and 5.5 % in the blade root moment in y axis, stationary hub moment in z axis and yaw bearing x and y moments respectively compared to the $C2$ control scheme. The load reduction in the tower base moment in x axis due to the reduction of the wind

Table 5.4 Fatigue load analysis

	m	$C1$	$C2$	$C3$	$C4$
Blade MFlap	12	100	100	102.1	98.6
Blade MEdge	12	100	100	100.1	99.5
Blade root Mx	12	100	99.9	100.0	101.0
Blade root My	12	100	98.8	98.9	91.3
Blade root Mz	12	100	98.3	101.0	99.0
Stationary hub Mx	9	100	100	99.8	99.0
Stationary hub My	9	100	99.2	99.6	92.8
Stationary hub Mz	9	100	99.9	101.0	94.0
Yaw bearing Mx	9	100	101.3	98.4	99.2
Yaw bearing My	9	100	99.2	99.3	93.9
Yaw bearing Mz	9	100	99.5	99.6	94.0
Tower base Mx	3	100	88.1	86.2	85.2
Tower base My	3	100	95.0	95.2	97
Tower base Mz	3	100	99.9	100.0	108.8

effect in the tower side-to-side first mode is a 2.9 % better using the IPC in $C4$ than with the generator torque control loop in $C2$. The control effort to align the rotor plane developed by the IPC of the $C4$ control scheme involves a load increment of 8.9 % in the tower base moment in z axis.

Lastly, Tables 5.5 and 5.6 show the extreme load analyses using the four control schemes. These analyses are very influenced by the activation and deactivation of the controllers, mainly of the IPC, when the wind turbine arrives to work in the above rated zone, so the results using IPC in $C4$ control scheme could be improved using better start-up strategies of the control system.

In the extreme DLC1.6 load case analysis, the blade root edgewise moment is hardly reduced due to the faster response of the collective pitch robust controller to regulate the generator speed. This rapidity also reduces other loads in blades, hub, yaw and tower. The $C3$ control strategy does not present important improvements compared to the $C2$ (only the blade root flapwise moment is reduced). On the other hand, the activation of the IPC in $C4$ control strategy involves important load reduction of 28.72 and 22.8 % compared to $C2$ in the DLC1.6 case in stationary hub moment in y axis and in the tower base moment in x axis respectively. Also, the $C4$ control strategy activation involves load increments in blade root moment in x axis, yaw bearing moment in z axis and tower base moment in z axis due to the extra-effort to align the rotor plane with the IPC.

The extreme load DLC1.9 analysis present important extreme load reductions in the x axis of the moments analyzed in Table 5.5 using the $C2$ control strategy compared to the $C1$. Also, the activation of the $C3$ control scheme with the collective pitch gain scheduled robust control improves the regulation of the

Table 5.5 Extreme load DLC1.6 analyses

	C1	C2	C3	C4
Generator speed	100	91.62	90.5	92.3
Blade MFlap	100	97.11	92.4	92.7
Blade MEdge	100	76.29	77.5	77.4
Blade root Mx	100	94.98	93.0	108.9
Blade root My	100	96.89	91.6	93.4
Blade root Mz	100	89.63	86.2	90.1
Stationary hub Mx	100	85.52	83.0	85.1
Stationary hub My	100	95.02	94.8	66.3
Stationary hub Mz	100	103.36	104.1	105.8
Yaw bearing Mx	100	86.00	84.9	87.3
Yaw bearing My	100	84.95	94.0	84.2
Yaw bearing Mz	100	106.36	105.6	115.5
Tower base Mx	100	87.92	85.7	65.1
Tower base My	100	98.60	97.5	98.8
Tower base Mz	100	106.34	105.6	115.4

Table 5.6 Extreme load DLC1.9 analyses

	C1	C2	C3	C4
Generator speed	100	100.59	95.6	100.7
Blade MFlap	100	100.18	94.7	95.5
Blade MEdge	100	101.66	97.7	99.3
Blade root Mx	100	99.14	97.5	97.1
Blade root My	100	99.81	94.3	95.0
Blade root Mz	100	100.45	89.6	107.4
Stationary hub Mx	100	99.05	99.0	98.9
Stationary hub My	100	99.31	89.7	56.0
Stationary hub Mz	100	90.95	103.9	98.1
Yaw bearing Mx	100	99.40	99.1	97.7
Yaw bearing My	100	104.31	94.1	93.4
Yaw bearing Mz	100	93.31	105.5	101.1
Tower base Mx	100	98.29	96.7	73.1
Tower base My	100	98.89	93.9	98.5
Tower base Mz	100	93.31	105.5	101.1

generator speed in 4.44 % but the loads are increased in the z axis in the different moments analyzed. The activation of the IPC in $C4$ reduces the loads in the stationary hub moment in y axis and tower base moment in x axis in 43.3 and 25.1 % respectively compared to the results using the $C2$ control scheme. In this extreme load analysis, the loads in blade root moment in z axis are increased using the $C4$ control strategy.

5.5 Conclusions

This chapter proposes one process to design different multivariable robust controllers for load mitigation in wind turbines. These controllers are compared with a baseline control strategy named $C1$, which is based on classical control methods used in wind turbines, not only in the controller design process, but also in the validation process with different complex analyses from simulations with the wind turbine non-linear model in GH Bladed. Some conclusions can be extracted from the work presented in this chapter:

- The control objectives of each control strategy are summarized in Table 5.1. The $C1$, $C2$ and $C3$ control strategies need a generator speed sensor and a tower top accelerometer to use them in the developed generator torque and collective pitch angle controllers. However, the $C4$ control strategy also needs blade root sensors to solve the specific control objectives including the IPC.
- The robustness of the generator torque and collective pitch controllers included in the $C2$ control scheme is carefully analyzed in Sect. 5.2. The mixed sensitivity problems to develop the controller syntheses are explained from the nominal plants to the definition of the weight functions. The proposed generator torque and collective pitch blade controllers perfectly mitigate the loads in the desired components of the wind turbine and they extract the nominal electric power value during the power production in the above rated zone.
- In the gain scheduled control included in $C3$ control scheme, the three LTI H_∞ controllers are perfectly interpolated without losing the stability and performance in all trajectories of the above rated zone solving an LMI system. These controllers perfectly improve the regulation of the generator speed compared with the LTI H_∞ controller in $C2$. The parameter adaptation in this gain scheduled controller is not optimized for gust inputs. Other variables with a faster response than the pitch angle signal, like generator speed error, can be taken into account to calculate the varying parameter value to improve the generator speed regulation in extreme wind gust cases.
- The multivariable robust IPC included in the $C4$ control strategy satisfies the proposed control objectives: to reduce the asymmetrical loads which appear in the rotor due to its misalignment and to mitigate the load in the tower reducing the wind effect in the tower side-to-side first mode. The load mitigation in the tower reducing the wind effect in the tower side-to-side first mode using the $C4$

control strategy improves the load reduction results comparing to the *C2* and *C1* baseline control strategies. Furthermore, the quality of the electrical power using the *C4* control strategy is better than using the *C2* control strategy because the tower side-to-side first mode damping is developed with an IPC instead of with a generator torque control. A start-up algorithm for the Individual Pitch Controller is necessary to have a softly activation of this control loop to reduce the extreme loads during the transition from the below rated to the above rated control zones.

- The designed feedback control strategies, which reduce the wind effect in some structural modes, mainly mitigate the fatigue loads in the wind turbine variables they are controlling. Other control loops like the rotor alignment and the generator speed regulator affect not only the variable they are trying to control. The effect of the increment of the bandwidth of the output sensitivity function in the generator speed regulation considerably affects the mitigation of the extreme loads. The collective pitch angle control responds quickly and the wind turbine rapidly changes the pitch angle in the blades to regulate the generator speed.
- The designed robust controllers have an important dependence from the nominal plants and these plants do not take into account the wind turbine rotational modes ($1P$, $3P$...) because they are not considered in the linearization process in GH Bladed. The robust control strategies can be improved if the plants consider these modes. This consideration can be developed by model identification from real data from the wind turbine or with complex analytical models.
- The proposed control strategies have been validated in GH Bladed for production and under extreme wind cases.

5.6 Future Work

Some of the work explained in this chapter has been towards numerical algorithms for the design of H_∞ and gain scheduled controllers. These algorithms are not totally matured and they need further research in different areas. The future work to continue with the work carried out in this chapter and to continue with the improvement of the load mitigation in wind turbines could be as follows:

- To use wind turbine models from the identification of real data of a wind turbine. These models are less ordered and the non-structural modes, like $1P$ or $3P$, are included in them. It is useful to design controllers to mitigate the wind effect in these modes and the computational cost to make the control synthesis will be smaller.
- To estimate the wind speed with a Kalman filter or other techniques, or to use LIDAR sensors. The inclusion of the wind speed measurement in the control strategies is an advantage because the main disturbance of the system can be

known. This wind input can be used to be varying parameter of the gain scheduled controllers to adapt quickly their dynamics to the present wind.

- To improve the individual pitch controllers. If the pitch actuator bandwidth increases, the performance of individual pitch controller would be better because the wind effect in the blade modes can be mitigated.
- To improve the gain scheduled controllers in the above rated zone including new operational points in the family of linear models when the wind turbine do not work in the operational points of the curve of power production (Fig. 5.1).
- To improve gain scheduled controllers for wind gust inputs including a new parameter dependence with a faster response than the pitch angle signal, like the generator speed error, to have a better generator speed regulation in extreme wind cases.

Acknowledgments The material used in this chapter was partly supported by the Spanish Ministry of Economy and Competitiveness and European FEDER funds (research project DPI2012-37363-C02-02).

References

1. Jonkman JM, Butterfield S, Musial W, Scott G (2009) Definition of a 5-MW reference wind turbine for offshore system development. NREL Technical Report NREL/TP-500-38060
2. Díaz de Corcuera A (2013) Design of robust controller for load reduction in wind turbines. Thesis. University of Mondragon, The Basque Country, Spain, 2013
3. Díaz de Corcuera A, Pujana-Arrese A, Ezquerria JM, Segurola E, Landaluze J (2012) H_∞ based control for load mitigation in wind turbines. *Energies* 2012(5):938–967
4. Díaz de Corcuera A, Nourdine S, Pujana-Arrese A, Camblong H, Landaluze J (2011) GH BLADED'S linear models based H-infinity controls for off-shore wind turbines. In: EWEA Offshore 2011. Nov 2011. Amsterdam (Holland)
5. Díaz de Corcuera A, Pujana-Arrese A, Ezquerria JM, Segurola E, Landaluze J (2012) Wind turbine load mitigation based on multivariable robust control and blade root sensors. In: *The Science of Making Torque from Wind*. October 2012. Oldenburg (Germany)
6. International Standard IEC 61400-1 Second Edition 1999-02 Wind turbine generator systems. Part 1: Safety requirements
7. Bossanyi EA (2000) The design of closed loop controllers for wind turbines. *Wind Energy* 3(3):149–163
8. Laks JH, Pao LY, Wright A (2009) Control of wind turbines: past, present, and future. In: *American control conference 2009*. June 2009. St. Louis (USA)
9. Pao LY, Johnson KE (2009) A tutorial on the dynamics and control of wind turbines and wind farms. In: *American control conference 2009*. June 2009. St. Louis (USA)
10. Bossanyi EA (2009) Controller for 5 MW reference turbine. European Upwind Project Report. www.upwind.eu. Accessed Feb 2013
11. Schaak P, Corten GP, van der Hooft EL (2003) Crossing resonance rotor speeds of wind turbines. ECN Wind Energy, Paper ECN-RX-03-041
12. Van der Hooft EL, Schaak P, van Engelen TG (2003) ECN Technical Report. DOWEC-F1W1-EH-03-0940

13. Caselitz P, Geyler M, Giebhart J, Panahandeh B (2011) Hardware-in-the-Loop development and testing of new pitch control algorithms. In: Proceeding of European wind energy conference and exhibition (EWEC), Brussels, Belgium, Mar 2011; pp 14–17
14. Johnson KE, Pao LY, Balas MJ, Kulkarni V, Fingersh LJ (2004) Stability analysis of an adaptive torque controller for variable speed wind turbines. In: Proceeding of IEEE conference on decision and control, Atlantis, Bahamas, Dec 2004; pp 14–17
15. Nourdine S, Díaz de Corcuera A, Camblong H, Landaluze J, Vecchiu I, Tapia G (2011) Control of wind turbines for frequency regulation and fatigue loads reduction. In: Proceeding of 6th Dubrovnik conference on sustainable development of energy, water and environment systems, Dubrovnik, Croatia, Sept 2011; pp 25–29
16. Sanz MG, Torres M (2004) Aerogenerador síncrono multipolar de velocidad variable y 1.5 MW de potencia: TWT1500. *Rev. Iberoamer. Automática Informática* 1:53–64
17. Bianchi FD, Battista HD, Mantz RJ (2007) Wind turbine control systems. In: Principles, modelling and gain scheduling design. Springer, London
18. Díaz de Corcuera A, Pujana-Arrese A, Ezquerro JM, Seguro E, Landaluze J (2013) Linear models based LPV (Linear parameter varying) control algorithms for wind turbines. *EWEA 2013*. Jan 2013. Vienna (Austria)
19. Geyler M, Caselitz P (2008) Robust multivariable pitch control design for load reduction on large wind turbines. *J Sol Energy Eng* 2008(130):12
20. Fleming PA, van Wingerden JW, Scholbrock AK, van der Veen G (2013) Field testing a wind turbine drivetrain/tower damper using advanced design and validation techniques. In: American control conference (ACC) 2013 (Washington: USA)
21. Iribas M, Landau (2009) Closed loop identification of wind turbines models for pitch control. In: 17th Mediterranean conference on control and automaton. June 2009. Thessaloniki (Greece)
22. Iribas M (2011) Wind turbine identification in closed loop operation. European Upwind Project Report. www.upwind.eu. Accessed Feb 2013
23. Garrad Hassan GL (2011) V4 Bladed Theory Manual. ©Garrad Hassan & Partners Ltd, Bristol
24. Jonkman JM, Marshall L, Buhl Jr (2005) FAST user's guide. NREL Technical Report NREL/TP-500-38230
25. Harris M, Hand M, Wright A (2005) LIDAR for turbine control. NREL Technical Report NREL/TP-500-39154
26. Van der Hooft EL, Schaak P, van Engelen TG (2003) Wind Turbine Control Algorithms; DOWEC-F1W1-EH-03094/0; Technical Report for ECN: Petten, The Netherlands, 2003
27. Ogata K (1993) *Ingeniería de Control Moderna*, 2 edn. Pearson Prentice Hall, Mexico
28. Bossanyi EA (2003) Wind turbine control for load reduction. *Wind Energy* 2003(6):229–244
29. Doyle JC, Francis BA, Tannenbaum AR (1992) *Feedback control theory*. MacMillan, New York
30. Scherer CW, El Ghaoui L, Niculescu S (eds) (2000) Robust mixed control and LPV control with full block scaling. In: Recent advances on LMI methods in control, SIAM (2000)
31. Balas G, Chiang R, Packard A, Safonov M (2010) Robust control toolbox. User's guide Mathworks. <http://www.mathworks.es/es/help/robust/index.html>. Accessed Feb 2013
32. Skogestad S, Postlethwaite I (2010) *Multivariable feedback control. Analysis and design*, 2 edn. Wiley, Chichester
33. Rugh WJ, Shamma JS (2000) Research on gain scheduling. *Automatica* 36(10):1401–1425
34. Bianchi FD, Mantz RJ, Christiansen CF (2004) Control of variable-speed wind turbines by LPV gain scheduling. *Wind Energy* 7(1):1–8
35. Díaz de Corcuera A, Pujana-Arrese A, Ezquerro JM, Seguro E, Landaluze J (2012) LPV model of wind turbines from GH Bladed's linear models. In: 26th European conference on modelling and simulation. ECMS 2012. May 2012. Koblenz (Germany)
36. Ostergaard KZ, Brath P, Stoustrup J (2008) Linear parameter varying control of wind turbines covering both partial load and full load conditions. *Int J Robust Nonlinear Control* 19:92–116

37. Bianchi FD, Sanchez Peña RS (2011) Interpolation for gain-scheduled control with guarantees. *Automatica* 47:239–243
38. Van Engelen TG, van del Hooft EL (2005) Individual pitch control inventory. ECN-C-030-138. Technical report for ECN. The Netherlands, 2005
39. Bossanyi EA, Wright A, Fleming P (2010) Controller field tests on the NREL CART2 Turbine. NREL/TP-5000-49085. Technical Report for NREL. Colorado, CO, USA, Dec 2010
40. Bossanyi EA, Wright A, Fleming P (2013) Validation of individual pitch control by field tests on two- and three-bladed wind turbines. *IEEE Trans Control Systems Technol* 21(2): 1067–1078
41. Stol KA, Zhao W, Wright AD (2006) Individual blade pitch control for the controls advanced research turbine (CART). *J Sol Energy Eng* 128(2):498–505
42. Wortmann S, (2010) REpower field test of active tower damping. In: European Upwind Project Report; Garrad Hassan & Partners Ltd., Bristol, UK
43. Heß F, Seyboth G (2010) Individual Pitch Control with tower side-to-side damping. In: Proceeding of 10th German wind energy conference, Bremen (Germany), Nov 2010
44. Nam Y (2011) Control system design, wind turbines. Ibrahim Al-Bahadly (ed), ISBN: 978-953-307-221-0
45. Coleman RP, Feingold AM (1957) Theory of self-excited mechanical oscillations of helicopter rotors with hinged blades. NASA TN 3844, NASA, 1957
46. Garrad Hassan GL (2011) V4 Bladed User Manual. ©Garrad Hassan & Partners Ltd, Chichester
47. Frandsen ST (2007) Turbulence and turbulence generated structural loading in wind turbine clusters. Ph.D. Thesis, Technical University of Denmark, Roskilde, Denmark, 2007
48. Söker H, Kaufeld N (2004) Introducing low cycle fatigue in IEC standard range pair spectra. In: Proceeding of 7th German wind energy conference, Wilhelmshaven, Germany, Oct 2004; pp 20–21